PHYSICAL REVIEW B **84**, 041202(R) (2011)

Origin of giant bulk Rashba splitting: Application to BiTeI

M. S. Bahramy,[1,*] R. Arita,[1,2] and N. Nagaosa[1,2]
[1]*Correlated Electron Research Group (CERG), RIKEN Advanced Science Institute, Wako, Saitama 351-0198, Japan*
[2]*Department of Applied Physics, University of Tokyo, Tokyo 113-8656, Japan*
(Received 8 May 2011; published 18 July 2011)

We theoretically propose the necessary conditions for realization of giant Rashba splitting in bulk systems. In addition to (i) the large atomic spin-orbit interaction in an inversion-asymmetric system, the following two conditions are further required; (ii) a narrow band gap, and (iii) the presence of top valence and bottom conduction bands of symmetrically the same character. As a representative example, using the first principles calculations, the recently discovered giant bulk Rashba splitting system BiTeI is shown to fully fulfill all these three conditions. Of particular importance, by predicting the correct crystal structure of BiTeI, different from what has been believed thus far, the third criterion is demonstrated to be met by a *negative* crystal field splitting of the top valence bands.

DOI: 10.1103/PhysRevB.84.041202 PACS number(s): 75.70.Tj, 31.15.A−, 71.15.−m, 71.28.+d

Exploiting the spin degree of freedom of the electrons is one of the primary goals in the rapidly growing field of spintronics. A promising candidate to achieve this goal is so-called Rashba effect, which relies on the spin-orbit interaction (SOI) of the carriers in an inversion (I) asymmetric environment.[1] This effect has been experimentally observed for a number of nonmagnetic metallic surfaces[2–4] and also demonstrated to exist at the interface of the semiconductor hetrostructures.[5] For most of these systems, the levels of Rashba spin splitting (RSS) are found to be rather small (at most several meV). However, there have been a few exceptions, e.g., the Bi-covered Ag(111) surface, for which the angle resolved photoemisson spectroscopy (ARPES) has revealed a giant RSS of the order of 200 meV.[3] Following these discoveries in two-dimensional situations, attempts have been made to realize RSS in three-dimensional systems, as such systems are expected to be an ideal laboratory for exploring many novel phenomena, e.g., the spin Hall effect and resonance-enhanced magneto-optical conductivity.

BiTeI, a polar layered semiconductor, has been very recently revisited from this point of view. The ARPES measurements clearly show a gigantic RSS among the lowest conduction bands (LCBs) in the bulk BiTeI,[6] leading to a substantial shift in the position of conduction band minimum (CBM), $k_{\mathrm{CBM}} = \pm 0.05$ Å^{-1}. The level of spin splitting obtained at CBM astonishingly reaches ∼400 meV, lying among the highest discovered so far. The corresponding Rashba energy $E_R = E_{\mathrm{CBM}} - E_0$, where E_0 indicates the energy of the two LCBs at their crossing point, is found to be over 100 meV. The spin-resolved ARPES measurements further reveal that these bands are fully spin-polarized, confirming the entire system is indeed subject to a giant RSS.[6]

Motivated by this discovery, we have performed a theoretical study based on the perturbative $\mathbf{k}\cdot\mathbf{p}$ formalism and backed by the first-principles calculations and group-theoretic analysis to investigate the origin of giant RSS in bulk materials. Through this study, we have identified three conditions required for realization of this intriguing phenomenon. These conditions are shown to be closely related to the relative ordering and symmetry character of the bands near Fermi level, E_F. As a representative case, BiTeI is shown to fully meet all these conditions, owing to its unusual electronic band structure near E_F.

As a starting point, we describe the general $\mathbf{k}\cdot\mathbf{p}$ Hamiltonian via perturbation theory (PT). Given the solution $H(\mathbf{k_0})$ at $\mathbf{k} = \mathbf{k_0}$, it can be expressed for nearby $\mathbf{k}$ as,

$$H(\mathbf{k}) = H(\mathbf{k_0}) + \frac{\hbar^2 q^2}{2m_0} + \frac{\hbar}{m_0}\mathbf{q}\cdot\mathbf{p} + H^{(1)} + H^{(2)} \quad (1)$$

where

$$H^{(1)} = \frac{\hbar^2}{4m_0^2c^2}(\nabla V \times \mathbf{q})\cdot\boldsymbol{\sigma}, \quad H^{(2)} = \frac{\hbar}{4m_0^2c^2}(\nabla V \times \mathbf{p})\cdot\boldsymbol{\sigma}. \quad (2)$$

Here, V, $\boldsymbol{\sigma}$, and $\mathbf{p}$ denote the crystal potential, Pauli matrices, and the momentum operator, respectively, and $\mathbf{q} = \mathbf{k} - \mathbf{k_0}$. Considering only the linear-in-k spin splittings, one can show that they can arise due to $H^{(1)}$ by the use of the first-order PT or the coupling between the perturbing terms $\frac{\hbar}{m_0}\mathbf{q}\cdot\mathbf{p}$ and $H^{(2)}$ in the second-order PT. The spin splitting arising from $H^{(1)}$ is, however, expected to be much less than that coming from $H^{(2)}$, and hence, unlikely to cause any giant RSS (i.e., $>$ 100 meV). This is because $H^{(1)}$ [$H^{(2)}$], as reflected by its $\mathbf{k}$-dependence ($\mathbf{p}$-dependence), originates from the crystal (atomic orbital) momentum. Since the velocity of the electron in its atomic orbit is far greater than the velocity of a wave packet, the spin splitting is accordingly expected to be strongly dominated by $H^{(2)}$.[7] The respective second-order perturbative correction in energy is given by[8,9]

$$\Delta\varepsilon_m^{(2)}(\mathbf{k}) = \frac{\hbar}{m_0}\sum_{n\neq m}\frac{\langle u_m|H^{(2)}|u_n\rangle\langle u_n|\mathbf{q}\cdot\mathbf{p}|u_m\rangle + \text{c.c.}}{\varepsilon_m - \varepsilon_n} \quad (3)$$

where u_i and ε_i are the eigenstate and eigenenergy corresponding to the state i at $\mathbf{k_0}$, respectively, and c.c. stands for the complex conjugation.

Equation (3) clearly indicates that the level of spin splitting is directly dependent on three conditions: (i) the strength of the spin-orbit interaction [represented by $H^{(2)}$], (ii) the energy difference between the neighboring states m and n, and (iii) the symmetry character of their corresponding eigenstates, determining if $\langle u_m|H^{(2)}|u_n\rangle$ is symmetrically allowed or not. In brief, states energetically close to each other and symmetrically

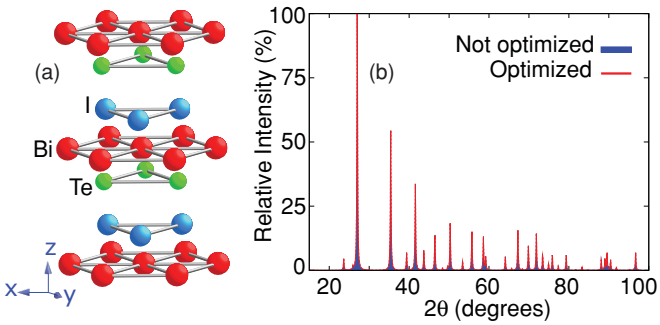

FIG. 1. (Color online) (a) Crystal structure of BiTeI and (b) simulated XRD pattern for the optimized and nonoptimized structures.

of the same character can effectively couple with each other and, hence, produce a large spin splitting, if the host atoms maintain a strong SOI. The first condition is, of course, a rather obvious requirement, already well-known in the context of surface RSS.[10] The other two are, however, less trivial and require more attention. In the case of semiconducting bulk materials, they can be satisfied if the band gap is sufficiently narrow and, more importantly, if both LCBs and the highest valence bands (HVBs) are symmetrically the same. The last condition requires an anomalous ordering of the bands near E_F, which is not usually allowed in conventional semiconductors. However, some polar semiconductors can exceptionally meet this criterion due to the *negative* crystal field splitting (CFS) of their top valence bands (TVBs). BiTeI is one such example, which in the following will be shown to fulfill all three conditions, thereby exhibiting a giant bulk RSS.

Having a trigonal structure with the space group $P3m1$ (No. 156), BiTeI is a polar compound in which Bi, Te, and I form stacking layers along the c axis. A characteristic feature of $P3m1$ group, as shown in Fig. 1(a), is the lack of I-symmetry. The highest symmetry operation allowed is C_{3v} along the c axis. The corresponding experimental lattice parameters a and c are 4.339 Å and 6.854 Å, respectively.[11] Assuming Bi to be at origin, Te and I have been experimentally proposed to be at (2/3,1/3,0.6928) and (1/3,2/3,0.2510) sites, respectively.[11] However, after a full structural optimization of atomic positions,[12] we have found that Te and I, surprisingly, change their positions to (2/3,1/3,0.7482) and (1/3,2/3,0.3076), respectively. In other words, our predicted Bi-Te (Bi-I) distance is exactly equal with the experimentally proposed Bi-I (Bi-Te) distance. Such a correction, as will be discussed later, leads to a number of fundamental changes in the electronic structure of BiTeI, including the appearance of a gigantic RSS, similar to what was observed by ARPES.[6] The failure of x-ray diffraction (XRD) experiment might be due to the fact that Te and I both have nearly the same ionic radii (133 pm and 131 pm, respectively) and atomic charges (52 and 53, respectively). Accordingly, they likely produce rather indistinguishable features in the XRD pattern. Indeed, the simulated XRD patterns,[13] as shown in Fig. 1(b), turn out to be nearly identical for both structures. Thus, the utilization of more sophisticated experimental techniques seems to be necessary for the proper identification of atomic positions in BiTeI. In the rest of this letter, we compare in detail the electronic structures of both the nonoptimized and optimized BiTeI, to asses if the above-mentioned conditions are indeed required for a giant bulk RSS.

Figure 2 shows the respective band structures for the both systems. In the absence of SOI, they show a semiconducting behavior with an energy gap $E_G \sim 1.2$ eV. As shown in Figs. 2(a) and 2(b), the lowest E_G is commonly found to be not at the Brillouin zone (BZ) center but at point $k_0 = A$, where $k_x = k_y = 0$ and $k_z = \pi/c$ [see Fig. 2(f)]. Up to 4 eV above E_F, the (6) conduction bands are predominated by Bi-6p states, whereas the Te-5p and I-5p most strongly contribute to the (12) valence bands down to -5 eV below E_F. Another important similarity is the presence of a rather large CFS among these bands. Without SOI, for any k-point other than those along Γ-A or the ones with accidental symmetry, all the p-type bands split into doubly degenerate bands. Along Γ-A, such states are allowed to form either two-fold or four-fold degenerate bands. Such a trend of CFS can be well described using the group theory. Within $P3m1$ group, at the BZ center and along Γ-A, all the k points have C_{3v} symmetry. Without spin, all the bands at A are thus transformed according to one of the single-group representations of C_{3v}.[14] Of our particular

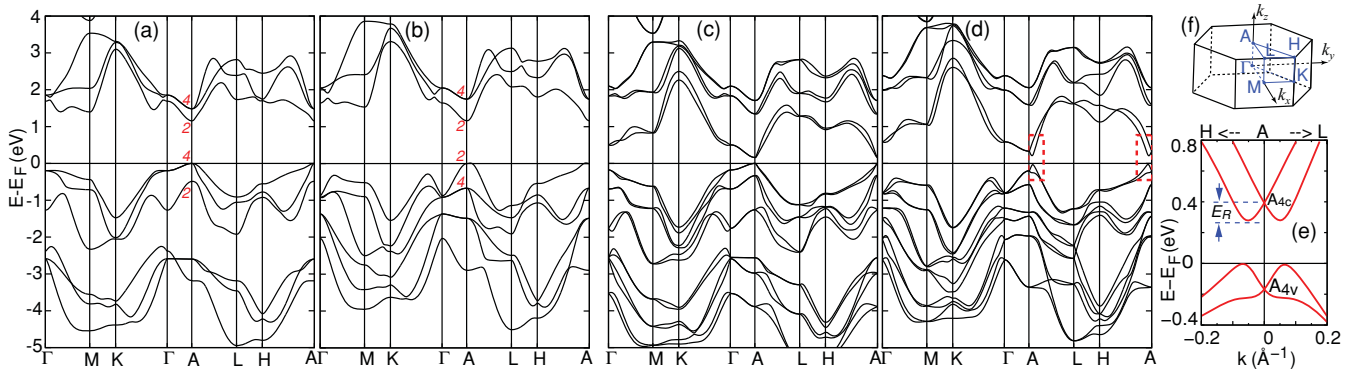

FIG. 2. (Color online) Calculated electronic band structures for the nonoptimized structure (a) without SOI and (c) with SOI and for the optimized structure (b) without SOI and (d) with SOI. (e) A scaled-up view of band dispersions along H-A-L direction for the optimized structure. (f) Corresponding high symmetry k points in the hexagonal Brillouin zone of BiTeI. In (a) and (b), the oblique numbers indicate the band degeneracies at point A for each structure (see the related discussion).

interest are $\{s, p_z\} \rightarrow A_1$ and $\{p_x, p_y\} \rightarrow A_3$, explaining why the p-type valence and conduction bands along Γ-A are either two-fold or four-fold degenerate. For the other internal BZ points, all the single representations are one-dimensional and hence nondegenerate except for spin.

Comparing the ordering of CFS of conduction bands at A, one notices a similar trend, that is, A_1–A_3 in the increasing order of energy. The same trend holds for TVBs in the nonoptimized structure. However, in the optimized structure, the ordering of TVBs is opposite, i.e., A_3–A_1 [see Fig. 2(b)]. This accordingly implies the existence of a *negative* CFS among this group of bands. As a result, both the LCBs and HVBs turn out to be A_1 (p_z) type and two-fold degenerate. It should be noted that such a negative CFS has already been observed for a number of chalcopyrite-type semiconductors, e.g., $CdSnP_2$[15] and $CuAlS_2$[16] as well as AlN.[17] The reason has been attributed to the strong ionicity of the atomic bondings, leading to a substantial structural distortion along their high symmetry axis.

Turning on SOI, the band structures undergo yet another drastic change. As shown in Figs. 2(c) and 2(d), E_G is closed down to ~ 0.28 eV, nearly five times smaller than that obtained without SOI. This is mainly due to the strong SOI of Bi, which shifts downward the $j = 1/2$ bands by nearly $-2\Delta_{\rm so}$, where $\Delta_{\rm so}$ denotes the atomic SOI energy (for Bi it is found to be ~ 0.5 eV). Despite this similarity, the trend of spin splitting near E_F is strikingly different between the two systems. A comparison between Figs. 2(c) and 2(d) clearly reveals that in the optimized structure a huge RSS takes place among both LCBs and HVBs at point A, whereas the nonoptimized structure fails to yield such a feature. As shown in Fig. 2(e), in the optimized structure, CBM and VBM are both shifted by nearly $k_{\rm CBM} = k_{\rm VBM} = \pm 0.05$ Å^{-1} from A in the (k_x,k_y) plane with an $E_R = 113$ meV, in excellent agreement with the ARPES data.[6] Such a good agreement is a strong indication that our predicted structure is indeed correct.

Having confirmed the existence of a giant RSS in bulk BiTeI, we next address the main question: whether this effect arises due to the fulfillment of the three conditions discussed earlier. As already might be understood, both the optimized and nonoptimized structures meet the first two criteria, namely the strong SOI in an I-asymmetric environment and narrow band gap. However, the last condition is only satisfied in the optimized structure as its LCBs and HVBs are symmetrically the same. To be more specific, upon introduction of SOI, the previously defined single-group representations A_1 and A_3 transform to their double group counterparts.[14] In C_{3v} space, the transformation is such that $A_1 \rightarrow A_4$ and $A_3 \rightarrow A_4 \oplus A_5 \oplus A_6$. In other words, A_1 transforms to A_4, whereas A_3 is split into two two-fold bands, A_4 and $A_5 \oplus A_6$ (the latter is hereafter simplified as $A_{5,6}$). Since TVBs of optimized structure undergo a negative CFS, the corresponding HVBs and LCBs are both of A_4 character. Figure 3 schematically shows the effects of CFS and SOI.

Turning back to Eqs. (1) and (2), one can use the method of invariants[9] to find an effective spin-splitting Hamiltonian linear in terms of k. For C_{3v} symmetry, it is easy to show that the only possible choice is $H_q \propto (\sigma_x q_y - \sigma_y q_x)$ because both (q_x,q_y) and (σ_x,σ_y) belong to the A_3 representation. H_q

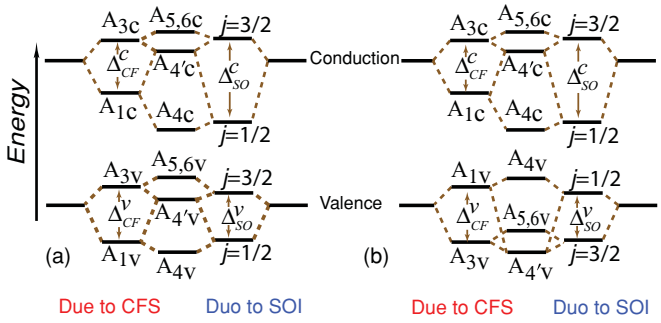

FIG. 3. (Color online) Diagrammatic representation of band splitting due to crystal-field splitting (CFS) and spin-orbit interaction (SOI) and their combination in (a) nonoptimized and (b) optimized BiTeI.

is clearly a Rashba-type Hamiltonian, giving the following spin-split energies $\Delta\varepsilon_m = \pm\alpha_m\sqrt{q_x^2 + q_y^2}$. As described in the beginning of this paper, $\Delta\varepsilon_m$ is expected to be dominated by $\Delta\varepsilon_m^{(2)}$. We can thus pursue with PT to qualitatively determine the second order correction in Rashba parameter α_m, denoted as $\alpha_m^{(2)}$. With the help of group theory, it turns out that in Eq. (3) $\langle u_m|H^{(2)}|u_n\rangle \neq 0$, if and only if both u_m and u_n are of A_4 character, implying that linear-in-k splitting is symmetrically forbidden for $A_{5,6}$ bands. Accordingly, we just need to consider $u_i = A_4$ and $A_{4'}$ (see Fig. 3). To derive an analytical form for $\alpha_m^{(2)}$ from Eq. (3), analogous to Gutche and Jane basis,[8,9,18] we define $|A_4\uparrow\downarrow\rangle = t\sqrt{\frac{1-w_4^2}{2}}|(x \pm iy)\downarrow\uparrow\rangle - w_4|Z\uparrow\downarrow\rangle$ and $|A_{4'}\uparrow\downarrow\rangle = t\frac{w_4}{\sqrt{2}}|(x \pm iy)\downarrow\uparrow\rangle + \sqrt{1-w_4^2}|Z\uparrow\downarrow\rangle$, where w_4 is to enforce the orthogonality of basis sets and t is equal with $+1(-1)$ for $|u_i\uparrow\rangle$ ($|u_i\downarrow\rangle$). The A_1-like basis $|Z\rangle$ is defined as $|Z\rangle = w_s|s\rangle + w_z|z\rangle$ with $w_s^2 + w_z^2 = 1$.

To simplify our derivations, we recall the fact that the states with small $(\varepsilon_m - \varepsilon_n)$ dominate $\Delta\varepsilon_m^{(2)}(\mathbf{k})$ and, thus $\alpha_m^{(2)}$. From Figs. 2(c) and 2(d), it is evident that $|\varepsilon_{4c} - \varepsilon_{4'c}| > 1.30$ eV and $|\varepsilon_{4v} - \varepsilon_{4'v}| > 1.15$ eV. On the other hand, for the optimized and nonoptimized structures, the respective $\Delta\varepsilon_{4,4} = \varepsilon_{4c} - \varepsilon_{4v}$ and $\Delta\varepsilon_{4,4'} = \varepsilon_{4c} - \varepsilon_{4'v}$ are both below 0.5 eV and very close to their E_G. Thus, as a good approximation for the former (latter), $\alpha_{4c}^{(2)} = \alpha_{4c,4v}^{(2)}$ ($\alpha_{4c}^{(2)} = \alpha_{4c,4'v}^{(2)}$), with

$$\alpha_{4c,4v}^{(2)} = \frac{\Delta_{4,4}}{\sqrt{2}\Delta\varepsilon_{4,4}}\left[w_{4v}\sqrt{1-w_{4c}^2}P_{x,Z} + w_{4c}\sqrt{1-w_{4v}^2}P_{Z,x}\right],$$
$$\alpha_{4c,4'v}^{(2)} = \frac{\Delta_{4,4'}}{\sqrt{2}\Delta\varepsilon_{4,4'}}\left[\sqrt{(1-w_{4v}^2)(1-w_{4c}^2)}P_{x,Z} - w_{4c}w_{4v}P_{Z,x}\right], \tag{4}$$

where $\Delta_{i,j} \equiv \langle A_{ic}\uparrow|H^{(2)}|A_{jv}\uparrow\rangle$ and $P_{x,Z} = -i\hbar\langle x_c|\partial/\partial x|Z_v\rangle$.

Constructing a set of maximally localized Wannier functions[19–21] for the conduction and valence bands around E_F, we have estimated w_{4v}^2 and w_{4c}^2 for the optimized and nonoptimized structures. For the latter, $w_{4v}^2 = 0.55$ and $w_{4c}^2 = 0.43$, both very close to the critical value 0.5. Assuming $P_{x,Z} = P_{Z,x}$, one can immediately find from Eq. (4) that $\alpha_{4c}^{(2)} \simeq 0$. Since $\alpha_{4'v,4c}^{(2)} = -\alpha_{4c,4'v}^{(2)}$, then $\alpha_{4'v}$ is also expected to be nearly zero. This clearly explains why the nonoptimized

structure shows almost no spin splitting among its HVBs and LCBs near point A. As for the optimized structure, the situation is completely different. Here, $w_{4v}^2 = 0.886$ and $w_{4c}^2 = 0.5$, implying that the HVBs are predominantly Z type. Consequently, $\alpha_{4c}^{(2)}$ and $\alpha_{4v}^{(2)}$ turn out to have appreciable values with equal magnitudes but opposite signs. In other words, under this situation, for both HVBs and LCBs, the absolute value of α can be nearly the same, but their signs are always opposite. That's exactly what we can see in the optimized BiTeI, as it also shows similar trend of spin-splitting among its LCBs and HVBs, such that their corresponding k_{CBM} and k_{VBM} are almost at the same place. Here, it is important to emphasize that such a second-order perturbative RSS is a direct result of an (i) anomalous ordering of top valence bands due to the existence of negative CFS, which allows the adjacent $A_{4\mathrm{v}}$ and $A_{4\mathrm{c}}$ to be symmetrically of the same character and, hence, to be coupled with each other thorough a perturbative Rashba-like Hamiltonian. Due to (ii) the large SOI of Bi leading to (iii) substantial band-gap narrowing, such a coupling can be effectively very strong. These are the three key factors for realization of giant RSS in BiTeI, and very likely any other giant bulk Rashba splitting material. For the other candidates, a negative CFS can either intrinsically exist due to the strong anisotropic ionicity of their atomic bondings or be externally produced, e.g., through a pressure-induced structural distortion.

In summary, in this study we combined the first-principles calculations with a group-theoretic analysis to investigate the origin of giant Rashba splitting in bulk systems. As a representative case, it was shown that in BiTeI, the interplay between the giant SOI of Bi and effectively large negative CFS of the TVBs led to a substantially strong coupling between the narrowly separated HVBs and LCBs via a perturbative Rashba-like Hamiltonian. Such conditions were expected to also be vital for realization of giant RSS in other bulk candidates.

This research is granted by the Japan Society for the Promotion of Science (JSPS) through the "Funding Program for World-Leading Innovative R&D on Science and Technology (FIRST Program)," initiated by the Council for Science and Technology Policy (CSTP).

*bahramy@riken.jp

[1] E. I. Rashba, Sov. Phys. Solid State **2**, 1109 (1960).

[2] S. LaShell, B. A. McDougall, and E. Jensen, Phys. Rev. Lett. **77**, 3419 (1996).

[3] C. R. Ast, J. Henk, A. Ernst, L. Moreschini, M. C. Falub, D. Pacile, P. Bruno, K. Kern, and M. Grioni, Phys. Rev. Lett. **98**, 186807 (2007).

[4] Y. M. Koroteev, G. Bihlmayer, J. E. Gayone, E. V. Chulkov, S. Blugel, P. M. Echenique, and P. Hofmann, Phys. Rev. Lett. **93**, 046403 (2004).

[5] J. Nitta, T. Akazaki, H. Takayanagi, and T. Enoki, Phys. Rev. Lett. **78**, 1335 (1997).

[6] K. Ishizaka, M. S. Bahramy, H. Murakawa, M. Sakano, T. Shimojima, T. Sonobe, K. Koizumi, S. Shin, H. Miyahara, A. Kimura, K. Miyamoto, T. Okuda, H. Namatame, M. Taniguchi, R. Arita, N. Nagaosa, K. Kobayashi, Y. Murakami, R. Kumai, Y. Kaneko, Y. Onose, and Y. Tokura, Nature Mater. **10**, 521 (2011).

[7] E. O. Kane, J. Phys. Chem. Solids **1**, 82 (1956).

[8] L. C. Lewyan Voon, M. Willatzen, M. Cardona, and N. E. Christensen, Phys. Rev. B **53**, 10703 (1996).

[9] L. C. Voon and M. Willatzen, *The k·p Method* (Springer, Berlin, 2009).

[10] M. Nagano, A. Kodama, T. Shishidou, and T. Oguchi, J. Phys. Condens. Matter **21**, 064239 (2009).

[11] A. V. Shevelkov, E. V. Dikarev, R. V. Shpanchenko, and B. A. Popovkin, J. Solid State Chem. **114**, 397 (1995).

[12] All the calculations reported here are carried out using PBE exchange-correlation functional and the augmented plane wave plus local orbitals method with inclusion of SOI as implemented in WIEN2K program (P. Blaha *et al*., URL: [http://www.wien2k.at]). The muffin tin radii are set to $R_{\mathrm{MT}} = 2.5$ bohr for all the atoms and the maximum modulus for the reciprocal vectors K_{max} is chosen such that $R_{\mathrm{MT}} K_{\mathrm{max}} = 7.0$. Accurate BZ samplings are performed using a $20 \times 20 \times 20$ k mesh. For the structural optimization, the stopping criterion is when the magnitude of force on all ionic sties is less than 0.1 mRy/bohr.

[13] Simulated by CRYSTALDIFFRACT program, Ver. 5.2.0: [http://www.crystalmaker.com/crystaldiffract/index.html].

[14] See Supplemental Material at http://link.aps.org/supplemental/10.1103/PhysRevB.84.041202 for a complete character table of the symmetry group C_{3v}.

[15] J. L. Shay, E. Buehler, and J. H. Wernick, Phys. Rev. Lett. **24**, 1301 (1970).

[16] V. Jayalakshmi, S. Davapriya, R. Murugan, and B. Palanivel, J. Phys. Chem. Solids **67**, 669 (2006).

[17] Y. Taniyasu, M. Kasu, and T. Makimoto, Appl. Phys. Lett. **90**, 261911 (2007).

[18] E. Gutsche and E. Jahne, Phys. Status Solidi **19**, 823 (1967).

[19] I. Souza, N. Marzari, and D. Vanderbilt, Phys. Rev. B **65**, 035109 (2001).

[20] A. A. Mostofi, J. R. Yates, Y. Lee, I. Souza, D. Vanderbilt, and N. Marzari, Comput. Phys. Commun. **78**, 685 (2008).

[21] J. Kuneš, R. Arita, P. Wissgott, A. Toschi, H. Ikeda, and K. Held, Comput. Phys. Commun. **181**, 1888 (2010).